ENG Transactions

Journal homepage: http://www.engtransactions.com

ENG Transactions, vol. 2, pp. 1-13, September 2021
ID: ENGT-2109152112394

Research Article

A New Lower Extremity Exoskeleton Composed of Parallel Robots for People with Lower Extremity Dyskinesia

Shuai Fan [1,2*], Guangyu Shen[1], Tao Liu[1], Guangkui Song[2], He Li[3]

[1] *School of Mechanical and Electrical Engineering, Chengdu University of Technology, Chengdu, Sichuan 610059, China*
[2] *Center for Robotics, University of Electronic Science and Technology of China, Chengdu, Sichuan 611731, China*
[3] *Centre for Marine Technology and Ocean Engineering (CENTEC), Instituto Superior Técnico, Universidade de Lisboa, Lisbon, Portugal*

Keywords

Exoskeleton,
Parallel robot,
Rehabilitation,
Variable stiffness.

Abstract

This paper contributes to the design of a new anthropomorphic lower extremity exoskeleton device inspired by the distribution of the lower extremity muscles. Different from traditional structures, where a single rotary actuator or a single linear actuator is installed at the joint, each leg of the designed exoskeleton device is a combination of two parallel robots. For the two parallel robots, one connects the waist, a thigh, and a shank to move the hip and knee joints, while, the other connects a thigh, a shank, and a foot to move the knee and ankle joints. In addition, a certain gap at the knee joint and the actuators with springs are also introduced as a basis to avoid the pain caused by the rigid structure. The results show that the new exoskeleton advantages in preforming higher control sensitivity, stronger bearing capacity, and better human-robot interaction performance compared with the previous prototypes.

1. Introduction

In recent years, the lower extremity exoskeleton (LEE) has been widely used to augment the strength of soldiers [1], [2], help patients with gait training [3], improve the athletic ability of elderly or muscular weakness [4, 30]. The LEEs as the medical devices have emerged in many large hospitals and rehabilitation centers to help patients with gait recovery. Nevertheless, these devices are expensive and require other auxiliary devices such as treadmills [5] and safety harnesses [4, 6], which are not accessible for all homes. Figure 1 shows two LEEs developed before, however, whose driving abilities are insufficient and the mechanism of which is too stiff resulting in a poor human-robot performance. Therefore, the main purpose of this paper is to design a LEE with high driving ability and good human-robot interaction performance.

* Corresponding Author: Shuai Fan
E-mail address: fansuai12345@163.com

Received: 1 September 2021; Revised: 19 September 2021; Accepted: 22 September 2021

Please cite this article as: S. Fan, G. Shen, T. Liu, G. Song, H. Li, "A New Lower Extremity Exoskeleton Composed of Parallel Robots for People with Lower Extremity Dyskinesia", ENG Transactions, vol. 2, pp. 1-13, 2021.

In general, LEEs can be structurally divided into two types: series and parallel. For the series LEEs, there is only one branch between two joints, and the actuator installed at the joint is often a rotating unit consisting of a motor and a gearbox, such as the HAL exoskeletons [4, 31], Rewalk robotics [7], Auto-LEE [8], WSE [9], Indego exoskeleton [10], and several others [2, 11]. The series LEEs are simple-structure, large range of motion, easy control. Since both the human body's gravity and external loads require the motor to withstand, the electrical actuator of series LEEs needs to provide a high torque, which results in a large structural size and only one active degree of freedom at each joint. Clearly, these results are not desired in the LEEs design. Hence, walking vehicles, safety harnesses, and crutches are used to share the effects of human body's gravity and external loads [4,7,9,32]. However, the walking vehicles and safety harnesses restricted LEESs' applications, and crutches require users have strong upper limbs, while, the strengths of many users are weaker. Thus, some parallel LEEs have gradually gained the attention of researchers. For the parallel LEEs, a minimum of two branches are used to distribution the human body's gravity and external loads, and the actuators is often a translational unit parallel to a constant link, such as the BLEEX [1], SJTU-EX [12], KIT-Exo-1 [33], ALEX [13], SAAM [14], APAL [15], and several others [16, 17, 18]. Comparing with the series LEEs, parallel LEEs have good load carrying characteristics, and most of parallel LEEs consist of only two branches, one of which is a constant link and another is a telescopic rod. Since the two branches are distributed on one side, such as the posterior or the lateral side of the leg, the inherent shortcoming of these devices is the unevenly distributed reaction force that will lead to instability of LEEs and increase the difficulty of control [33, 19, 20]. Accordingly, one of the purposes of this paper is to propose a new exoskeleton with stronger bearing capacity and uniformly distributed reaction forces to make the LEE bear most of the load and to improve the unevenly distributed reaction force.

On the other hand, the previous devices had poor human-robot interaction performance during walking due to the previous LEEs are stiff. In addition to the hysteresis of the control system, another important reason is that the stiffness of the muscle and ligament system is changeable with environments [21, 22]. In order to solve this problem, new LEEs with compliant actuators have been developed in recent years, such as LOPES [34,23], Mindwalker [35], KIT-EXO-1 [33], ATLAS [24], RTCA [25], PAM [26], and several others [27, 28]. Usually, these devices are primarily nested in the actuators that can be divided into a rotary actuator unit and a linear actuator unit. Hence, another purpose of this paper is to introduce a variable stiffness device to improve human-robot interaction performance during walking.

The main framework of this paper is as follows. The structure design and stiffness design of the proposed LEE are presented in Section 2 and Section 3, respectively. Next, the numerical simulations and discussion are given in the Section 4. Finally, the conclusions are drawn in Section 5.

Figure 1. Two previous LEE prototypes in our laboratory

2. Structure Design

2.1. Human Lower Extremity Motion System

As shown in Figure 2, the distribution of human lower limb muscles is obtained by Zygote Body software. Clearly, the thigh muscle consists of an anterior, posterior, and inner groups. The thigh anterior muscle group (TAMG) flexes the thigh and flexes the shank, the thigh posterior muscle group (TPMG) cause the extension of the hip joint and the flexion of the knee joint, and the thigh inner muscle group (TIMG) play the role of allowing the thigh to adduct and external rotation. Similarly, the shank muscles consist of an anterior, posterior and lateral groups. The shank anterior muscle group (SAMG) cause the dorsiflexion and varus of the foot, the shank lateral muscle group (SLMG) cause the valgus of the foot and the flexion of the toe, and the shank posterior muscle group (SPMG) mainly play the toe flexion and flexion of the knee joint. According to the muscle distribution and function of the human lower limb muscle system, four characteristics of the human lower extremity motion system can be obtained as follows:

(a) The flexion and extension of each joint are driven by different muscle groups, respectively.

(b) During human locomotion, the sagittal plane is the dominant plane of motion, and the anterior and posterior muscle groups are the dominant actuators.

(c) The femur and tibia of the leg serve to support the body's gravity, and their lengths are fixed.

(d) The thigh muscle system is connected to the waist, thigh and shank, and the shank muscle system is connected to the thigh, shank and foot.

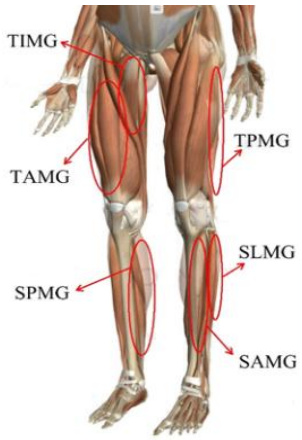

Figure 2. Human lower extremity

2.2. An Anthropomorphic Lower Extremity Exoskeleton

According to the mentioned four characteristics of the human lower extremity motion system, a new anthropomorphic LEE inspired by muscle distribution of human motion system called I-LEE (lower extremity exoskeleton inspired by muscle system) is developed as shown in Figure 3. The I-LEE consist of two identical legs, and each leg of the I-LEE is composed of two parallel robots called the thigh parallel robot and the shank parallel robot. The thigh parallel robot consists of a waist gasket, a thigh anterior chain (TAC), a thigh posterior chain (TPC), a thigh lateral chain (TLC) and a shank gasket. The shank parallel robot consists of a thigh gasket, a shank anterior chain (SAC), a shank posterior chain (SPC), a shank lateral chain (SLC) and a foot plate. The proposed LEE is synchronized with the human body movement through one waist gasket, two thigh gaskets, two shank gaskets and two foot plates. Clearly, the TAC, TPC, TLC, SAC, SPC and SLC of the proposed I-LEE mimic the distribution and function of the TAMG, TPMG, femur, SAMG, SPMG and tibia of the human body, respectively. Since the

anterior and posterior muscle groups are the dominant actuators of motion during human locomotion, the basic movement of the human body in the sagittal plane can be achieved by the proposed LEE.

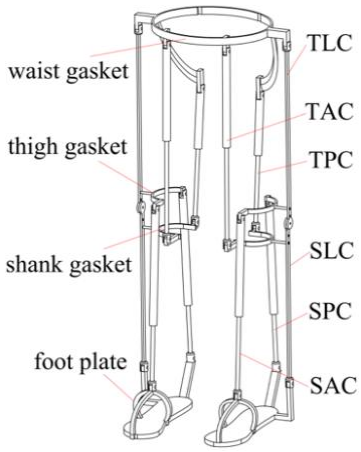

Figure 3. Structure of the I-LEE

As shown in Figure 4, the thigh parallel robot and the shank parallel robot are the RR+2RPR type parallel robots, where R denote the revolute joint, and P denote the prismatic joint. The foot plate is connected with the thigh gasket by three chains: SAC, SPC and SLC. The SAC and the SPC are in the same plane, and both of them are the RPR type. The SLC is the RR type, and its link is fixed with the shank gasket. Similarly, the shank gasket is connected with the waist gasket by three chains: TAC, TPC and TLC. The SAC and the SPC are also in the same plane, and both of them are the RPR type. The SLC is also the RR type, and its link is fixed with the thigh gasket. Clearly, the thigh parallel robot connects the waist, the thigh, and the shank, and the shank parallel robot connects the thigh, the shank, and the foot. It is note that the SAC and the SPC are not in the same plane as the TAC and TPC, but the SLC and the TLC are in the same plane.

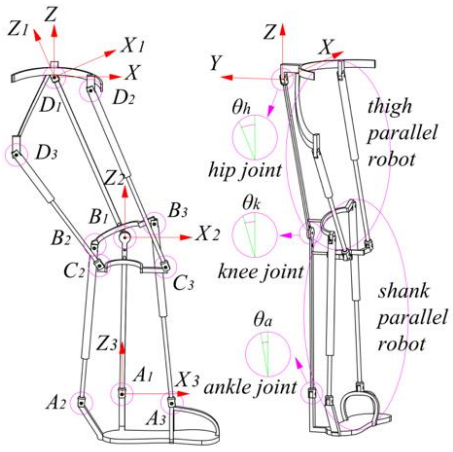

Figure 4. Muscle systems of the human lower extremity

2.3. Degree of Freedom and Control Strategy

Since the rotation axes of all the revolute joints are parallel to each other, the degree of freedom (DOF) of the proposed LEE can be determined by the Kutzbach Grubler criterion as

$$M = 3(n - g - 1) + \sum_{i=1}^{g} f_i = 3\times(12-15-1)+15=3 \quad (1)$$

It is not difficult to find that the obtained three DOFs are rotational degrees of freedom, and the three DOFs correspond to the rotational motion of the ankle, knee and hip joints in the sagittal plane, respectively. On the other hand, the DOF of the thigh parallel robot or shank parallel robot can also be obtained by the Kutzbach Grubler criterion as

$$M = 3(n - g - 1) + \sum_{i=1}^{g} f_i = 3\times(7-8-1)+8=2 \quad (2)$$

When one of the thigh or shank parallel robots is actively controlled and another becomes passive, the I-LEE has two active DOFs and one passive DOF. Namely, if the thigh parallel robot is active but the shank parallel robot is passive, the hip and knee joints are active but the ankle joint is passive, and, if the shank parallel robot is active but the thigh parallel robot is passive, the ankle and knee joints are active but the hip joint is passive.

As shown in Tab. 1 and Figure 5, the control strategy idea is given, and thigh and shank parallel robots can be separately controlled during human locomotion to achieve the purpose of controlling different joints. When the travel speed is faster, the thigh parallel robot is active but the shank parallel robot is passive for the swing leg of the I-LEE, and the thigh parallel robot is passive but the shank parallel robot is active for the support leg of the I-LEE. In other word, the hip and knee joints of the swing leg of the I-LEE are active but the ankle joint of the swing leg of the I-LEE is passive, and the ankle and knee joints of the support leg of the I-LEE are active but the hip joint of the support leg of the I-LEE is passive. When the travel speed is slow or the user is standing, both of the thigh and shank parallel robots are active. In this situation, all of the hip joints, knee joints and ankle joints are controlled by the I-LEE. Hence, this design allows for different strategies to accommodate different training requirements and different levels of dyskinesia.

Table 1. Control Strategy

	Hip joint	Knee joint	Ankle joint
support leg of the faster travel	passive	active	active
swing leg of the faster travel	active	active	passive
standing or low speed	active	active	active

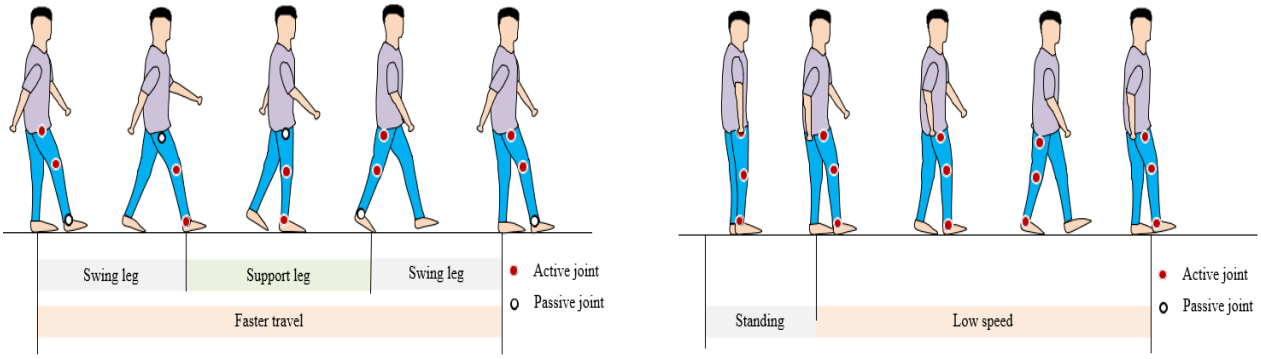

Figure 5. Control strategy of different phases

2.4. Kinematics

Figure 4 shows the kinematic model and a reference frame D_1 – XYZ(0^{th} reference frame) with an origin located at the position of the hip joint. The Y-axis is defined as the direction of advancement, the direction of the Z-axis is vertically upward, and the direction of the X-axis is determined by the right-hand rule. If the hip, knee and ankle angles are denoted by θ_h, θ_k and θ_a, the reference frame D_1–$X_1Y_1Z_1$ (1^{th} reference frame) can be obtained by rotating the 0^{th} reference frame by θ_h around the Y-axis, the reference frame B_1–$X_2Y_2Z_2$ (2^{th} reference frame) can be obtained by rotating the1^{th} reference frame by θ_k around the Y-axis and shifting the origin to B_1 point, and the reference frame A_1–$X_3Y_3Z_3$ (3^{th} reference frame) can be obtained by rotating the2^{th}reference frame by θ_a around the Y-axis and shifting the origin to A_1 point. When the travel speed is faster, for the support leg, the knee and ankle joints are active but the hip joint is passive, so that the lengths of the SPC and SAC are constrained but the lengths of the TPC and TAC are free. In this situation, θ_a and θ_k are given, and the constraint equations associated with two active limbs of the shank parallel robot can be expressed in the 0^{th} reference frame as

$$\begin{cases} L_{SPC} = |R_{(-\theta_a)}[0,0,l_{SLC}]^T + R(-\theta_k)B_2 - A_2| \\ L_{SAC} = |R_{(-\theta_a)}[0,0,l_{SLC}]^T + R(-\theta_k)B_3 - A_3| \end{cases} \tag{3}$$

where l_{SLC} is the length of the SLC, $\boldsymbol{B}_2$ and $\boldsymbol{B}_3$ are the locations in the 2^{th} reference frame of two end points of the SPC and SAC connected with the thigh gasket, respectively, A_2 and A_3 are the locations in the 3^{th} reference frame of two end points of the SPC and SAC connected with the foot plate, respectively, and

$$\boldsymbol{R}_{(\theta)} = \begin{pmatrix} \cos(\theta) & 0 & \sin(\theta) \\ 0 & 1 & 0 \\ -\sin(\theta) & 0 & \cos(\theta) \end{pmatrix} \tag{4}$$

For the swing leg, the hip and knee joints are active but the ankle joint is passive, so that the lengths of the TPC and TAC are constrained but the lengths of the SPC and SAC are free. In this situation, θ_h and θ_k are given, and the constraint equations associated with two active limbs of the shank parallel robot can be expressed in the 3^{th} reference frame as

$$\begin{cases} L_{TPC} = |R_{(\theta_h)}[0,0,l_{TLC}]^T + R(\theta_k)C_2 - D_2| \\ L_{TAC} = |R_{(\theta_h)}[0,0,l_{TLC}]^T + R(\theta_k)C_3 - D_3| \end{cases} \tag{5}$$

where l_{TLC} is the length of the TLC, C_2 and C_3 are the locations in the 2^{th} reference frame of two end points of the TPC and TAC connected with the shank gasket, respectively, and $\boldsymbol{D}_2$ and $\boldsymbol{D}_3$ are the locations in the 0^{th} reference frame of two end points of the TPC and TAC connected with the waist gasket, respectively.

For the standing or low speed phase, all of the hip, knee and ankle joints are active, so that all the lengths of the TPC, TAC, SPC and SAC are constrained. In the 0^{th} reference frame, if θ_h, θ_k and θ_a are given, the constraint equations associated with two limbs of the thigh parallel robot are same with the Eq. (3), and the constraint equations associated with two limbs of the shank parallel robot are same with the Eq. (5).

3. Compliance Design

3.1. An Anthropomorphic Compliance System

As shown in Figure 6, the role of the meniscus is to increase the stability of the knee joint and to cushion the shock during walking, jumping or running. At the same time, some studies have shown that the stiffness of the muscle system of the lower extremities varies in different environments [25]. As a result, the shank parallel robot is optimized in structure for performance of variable stiffness. As shown in Figure 7, three measures are used to improve the stiffness performance of the I-LEE as follows:

(a) The knee joint has a small gap filled with elastic medium.

(b) A spring is placed between the foot plate and the cylinder of the SAC, and two ends of the spring are free.

(c) A springs is placed in the cylinder of the SPC, and two ends of the spring are free.

3.2. Compliance of the Shank Parallel Robot

For the shank parallel robot, the stiffness model can be expressed based on the virtual work principle as

$$\Delta\theta = KF \tag{6}$$

$$K = J^T \begin{bmatrix} 1/k_{SPC} & 0 \\ 0 & 1/k_{SAC} \end{bmatrix} J \tag{7}$$

where K is the compliance matrix, k_{SPC} is the stiffness of the SPC, k_{SAC} is the stiffness of the SAC, and J is the Jacobian matrix. According to the kinematic analysis, the Jacobian matrix can be obtained by the derivative operation of the kinematic constraint equation, and the stiffness of the SPC and SAC can be obtained as follows.

Figure 6. Human knee joint

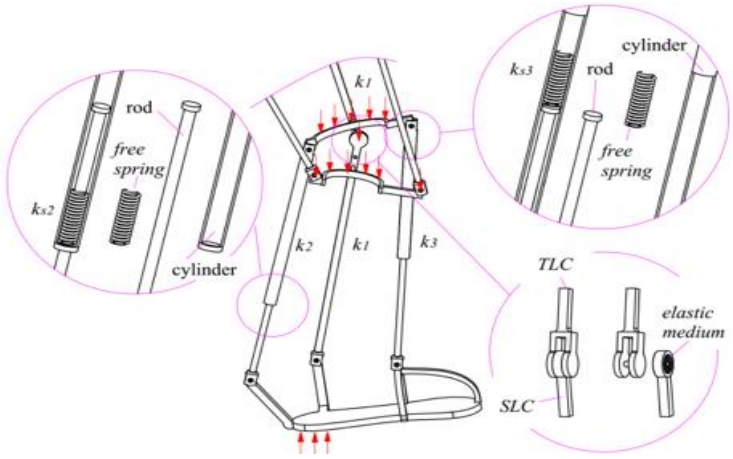

Figure 7. Structure with springs

For the SPC of the shank parallel robot, when the length of the SPC is shorter than a critical length denoted by l_{cri}^{SPC}, the spring will not work. In this situation, if the stiffness of link of SPC is k_2, the stiffness of the SPC can be expressed by

$$\begin{cases} k_{SPC} = k_2 \\ l_{SPC} \le l_{cri}^{SPC} \end{cases} \tag{8}$$

However, if the length of the SPC is longer than the critical length, the spring will work. Figure 8. is shown the variable stiffness principle [29], and the geometric dimension constraints can be expressed as

$$\begin{cases} l_0 = x_0 + a_0 \\ l_0 + \Delta l = x_0 + \Delta x + a_0 + \Delta a \end{cases} \tag{9}$$

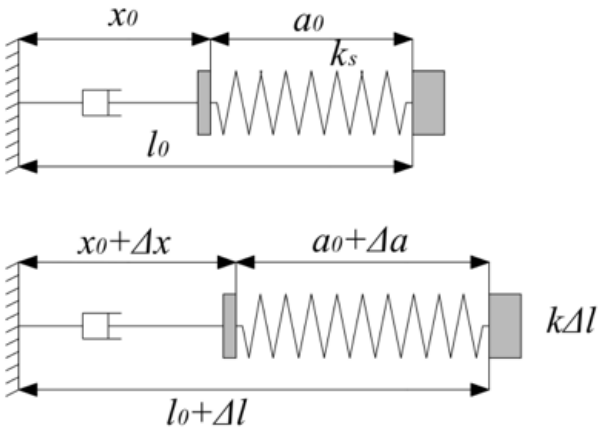

Figure 8. Geometric dimension constraints of deformations

where l_0, x_0 and a_0 are the initial length of the chain, the actuator and the spring, respectively, and Δl, Δx and Δa are the tiny deformation of the chain, the actuator and the spring, respectively. If the stiffness of this spring is k_s and the stiffness of this chain is k, we have $k_s \Delta a$ = k Δl. Since $\Delta l = \Delta x + \Delta a$, thus,

$$k = \frac{\Delta l - \Delta x}{\Delta l} k_s \tag{10}$$

Therefore, the stiffness of the SPC can be expressed by

$$\begin{cases} k_{SPC} = k_2, l_{SPC} \geq l_{cri}^{SPC} \\ k_{SPC} = \frac{\Delta l_{SPC} - \Delta x_2}{\Delta l_{SPC}}, l_{SPC} \leq l_{cri}^{SAC} \end{cases} \tag{11}$$

or the SAC of the shank parallel robot, when the length of the SPC is longer than a critical length denoted by l_{cri}^{SAC}, the spring will not work, and, when the length of the SPC is shorter than the critical length, the spring will work. In this situation, if the stiffness of link of SPC is k_3, the stiffness of the SAC can be expressed by

$$\begin{cases} k_{SAC} = \frac{\Delta l_{SAC} - \Delta x_3}{\Delta l_{SAC}}, l_{SAC} \leq l_{cri}^{SAC} \\ k_{SAC} = k_3, l_{SPC} \geq l_{cri}^{SPC} \end{cases} \tag{12}$$

4. Discussion and Result

In this section, the Clinical Gait Analysis (CGA) data are utilized to verify the practicability of the proposed I-LEE and these data are obtained by a normal person weighing 70kg with a travel speed of 0.5m/s. The Figure 9. shows the changes of three angles of the hip, knee and ankle during a gait cycle. It is worth noting that we assume that the I-LEE has a low speed in the following examples, which means that all joints are active. Meanwhile, the length and stiffness of the placed spring are directly given. Obviously, different given values will directly affect the stiffness performance of the proposed robot, but it is not discussed in detail due to space limitations.

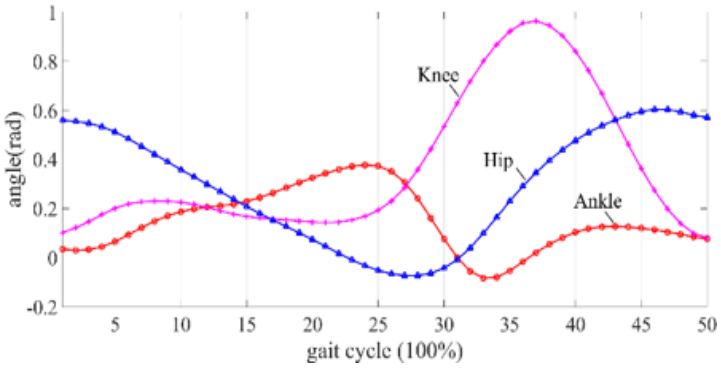

Figure 9. Angel data of the CGA

4.1. Numerical Example

In the simulations, the point locations are

$$\begin{cases} \boldsymbol{A}_2 = [-100, -100, 0]^T \\ \boldsymbol{B}_2 = [-200, -100, 50]^T \\ \boldsymbol{C}_2 = [-200, -50, -50]^T \\ \boldsymbol{A}_3 = [100, -100, 0]^T \\ \boldsymbol{B}_3 = [200, -100, 50]^T \\ \boldsymbol{C}_3 = [200, -50, -50]^T \end{cases}, \tag{13}$$

and the unit is millimeters (mm). l_{TLC} and l_{SLC} are 470 mm and 370 mm, respectively. Based on the CGA data and the kinematics model, the lengths of two active chains of the the thigh parallel robot are obtained as shown in Figure 10, and the lengths of two active chains of the shank parallel robot are obtained as shown in Figure 11.

According to the result of the kinematic simulation, the critical length of the SPC is 460 mm, and the critical length of the SAC is 400 mm. The elastic module of the hydraulic oil is 1.5×10^9 and the stiffness of the spring is 1.3×10^5 N/m. As shown in Figure 12. he minimum eigenvalue of the compliance matrix given in Eq. (7) are obtained, where the effects of the spring are ignored in Figure 12. and considered in Figure 13.

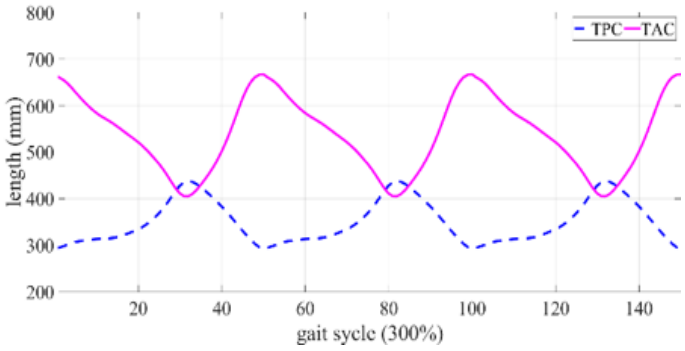

Figure 10. Lengths of active chains of thigh parallel robots

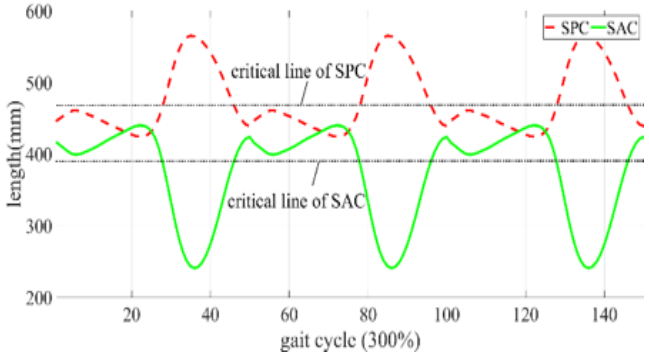

Figure 11. Lengths of active chains of shank parallel robots

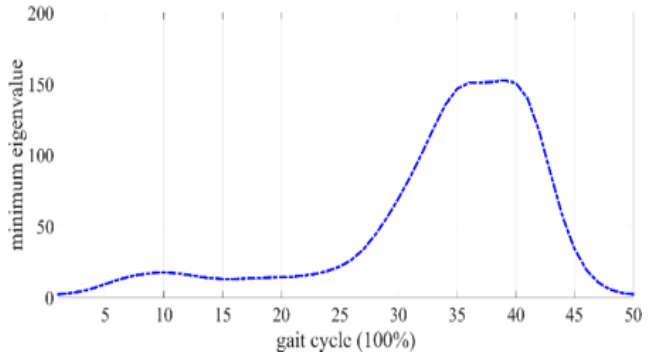

Figure 12. Compliance indexes of the I-LEE with springs

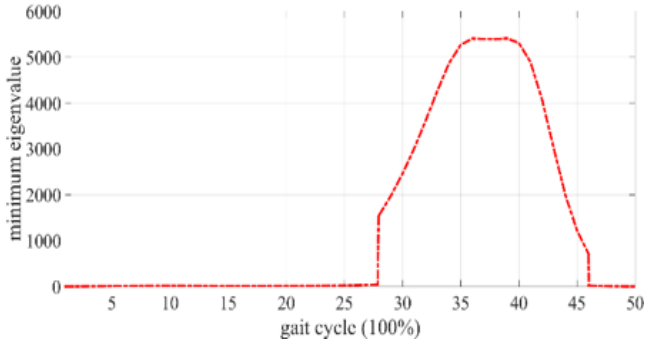

Figure 13. Compliance indexes of the I-LEE with springs

4.2. Comparisons

The second prototype in our laboratory called traditional LEE is used in this section, and the knee joint of the traditional LEE is driven by a hydraulic actuators. Firstly, the comparisons of the change in the active chain length of the traditional LEE and the change in the length of the I-LEE during three cycles are shown in Figure 14. and Figure 15. The lengths of the active chain of TPC, TAC, SPC and SAC of the I-LEE vary 150 mm, 260 mm, 140 mm and 200 mm, respectively, while the length of the active chain of the traditional LEE varies by 20 mm. Obviously, the active chains of the proposed I-LEE has a better range of variation, and roughly seven times that of traditional robots.

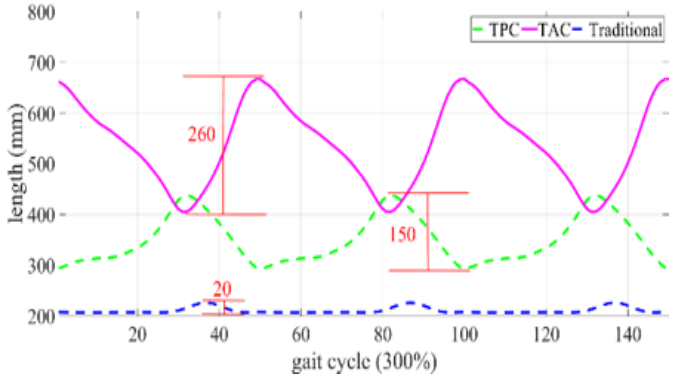

Figure 14. Sensitivity comparison of active chains of thigh parallel robots

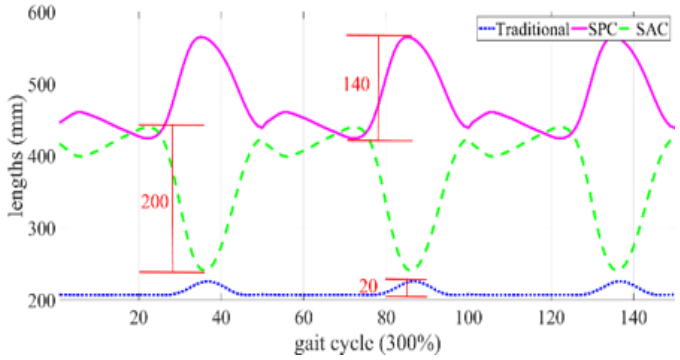

Figure 15. Sensitivity comparison of active chains of shank parallel robots

On the other hand, the compliance comparisons of the shank parallel robot of the I-LEE with springs, the shank parallel robot of the I-LEE without springs and the traditional LEE are drawn in Figure 16. In one gait cycle, the maximum of the minimum eigenvalues of the compliance matrix of the I-LEE with springs, the traditional LEE and the I-LEE without springs are 5398, 1180, and 160, respectively.

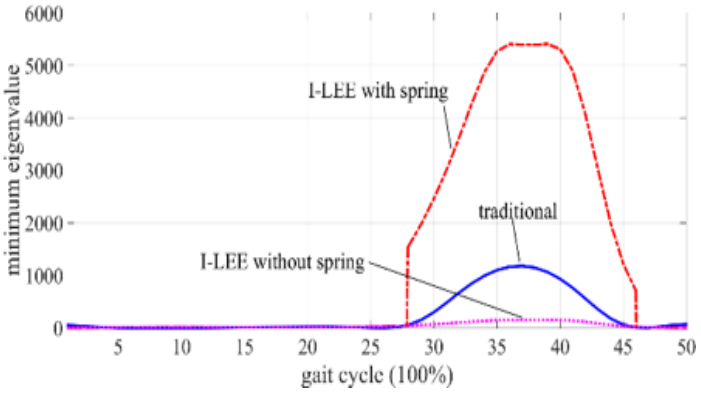

Figure 16. Compliance comparisons

4.3. Result

Firstly, a larger change interval means that the more precise the control, the precision and sensitivity of the control are higher, so the proposed I-LEE has better sensitivity than the traditional LEE. Secondly, the smaller eigenvalue denote that the joints are stiffer, and the larger eigenvalue indicate that the joints are more compliant. Based on the compliance comparisons, we can find that the proposed I-LEE without springs has worse flexibility than the traditional robot but the proposed I-LEE with springs has better flexibility than the traditional robot. Hence, the I-LEE has a better human-robot interaction performance compared with the previous prototypes. Finally, since each leg of the proposed LEE has three branches, the I-LEE has a stronger bearing capacity than traditional LEEs and its reaction forces are uniformly distributed.

5. Conclusions

In order to overcome the main shortcomings in the previous prototypes, a new anthropomorphic lower extremity exoskeleton inspired by the distribution of the lower extremity muscles is proposed in this paper. Design inspiration, structure, kinematics, control ideas, and compliance design concepts of the proposed LEE are discussed in this article. Overall, the advantages of the proposed LEE can be summarized as: more anthropomorphic design, higher sensitivity, better human-robot interaction performance (better flexibility), stronger bearing capacity, and uniformly distributed reaction forces. However, the control strategy and the compliance design concepts are only a brief mention, the effects of the elastic medium are ignored, the stiffness of the SLC and thigh parallel robot are not considered, and the weight of the I-LEE is also a serious problem. In the future work, a prototype of the I-LEE will be produced, and then some detail performance will be investigated subsequently.

Acknowledgements

This work was supported by the National Natural Science Foundation of China [grant numbers: 51875086].

References

[1] H. Kazerooni, R. Steger, “The berkeley lower extremity exoskeleton,” *J. Dyn. Syst. Meas. Control-Trans. ASME*, vol. 128, pp. 14-25, 2006.

[2] K. H. Low, X.P. Liu, C.H. Goh, H.Y. Yu, “Locomotive control of a wearable lower exoskeleton for walking enhancement,” *J. Vib. Control*, vol. 12, pp. 1311-1336, 2006.

[3] Z.F. Lerner, D.L. Damiano and T.C. Bulea, “A lower-extremity exoskeleton improves knee extension in children with crouch gait from cerebral palsy,” Sci. Transl. Med., vol. 9, pp.1-10, 2007.

[4] S. Kubota, T. Abe, H. Kadone, Y. Shimizu, T. Funayama, H. Watanabe, A. Marushima, M. Koda, Y. Hada, Y. Sankai, M. Yamazaki, “Hybrid assistive limb (HAL) treatment for patients with severe thoracic myelopathy due to ossification of the posterior longitudinal ligament (OPLL) in the postoperative acute/subacute phase: A clinical trial,” *J. Spinal. cord. Med.*, vol. 42, pp. 517-525, 2019.

[5] Z.F. Lerner, D.L. Damiano, T.C. Bulea, “The Effects of Exoskeleton Assisted Knee Extension on Lower-Extremity Gait Kinematics, Kinetics, and Muscle Activity in Children with Cerebral Palsy,” *Sci. Rep*, vol. 7, pp.1-12, 2017.

[6] Z.F. Lerner, T.A. Harvey and J.L. Lawson, “A Battery-Powered Ankle Exoskeleton Improves Gait Mechanics in a Feasibility Study of Individuals with Cerebral Palsy,” *Ann. Biomed. Eng.*, vol. 47, pp. 1345-1356, 2019.

[7] A. Esquenazi, M. Talaty, A. Packel and M. Saulino, “The ReWalk Powered Exoskeleton to Restore Ambulatory Function to Individuals with Thoracic-Level Motor-Complete Spinal Cord Injury,” *Am. J. Phys. Med. Rehabil.*, vol. 91, pp. 911-921, 2012.

[8] Y. He, N. Li, C. Wang, L.Q. Xia, X. Yong and X.Y. Wu, “Development of a novel autonomous lower extremity exoskeleton robot for walking assistance,” *Front. Inform. Technol. Elect. Eng.*, vol. 20, pp. 318-329, 2019.

[9] U. Onen, F.M. Botsali, M. Kalyoncu, M. Tinkir, N. Yilmaz and Y. Sahin, “Design and Actuator Selection of a Lower Extremity Exoskeleton,” *IEEE-ASME Trans. Mechatron.*, vol. 19, pp. 623-632, 2014.

[10] C. Tefertiller, K. Hays, J. Jones, A. Jayaraman, C. Hartigan, T. Bushnik, G.F. Forrest, "Initial Outcomes from a Multicenter Study Utilizing the Indego Powered Exoskeleton in Spinal Cord Injury," *Top. Spinal. Cord Inj. Rehabi.*, vol. 24, pp. 78-85, 2018.

[11] A. Esquenazi and M. Talaty, "Robotics for Lower Limb Rehabilitation," *Phys. Med. Rehabil. Clin. N. Am.*, vol. 30, pp. 1-13, 2019.

[12] Y.J. Miao, F. Gao and D.L. Pan, Mechanical design of a hybrid leg exoskeleton to augment load-carrying for walking," *Int. J. Adv. Robot. Syst.*, vol. 10, pp. 1-11, 2013.

[13] S.K. Banala, S.H. Kim, S.K. Agrawal, J.P. Scholz, "Robot assisted gait training with active leg exoskeleton (ALEX)," *IEEE Trans. Neural Syst. Rehabil. Eng.*, vol. 17, pp. 2-8, 2009.

[14] W.Y. Liang, Y. Yu, "Manipulability inclusive principle for assistive resul evaluation of assistive mechanism," *J. Healthc. Eng.*, pp. 1-16, 2018.

[15] F.S. Zha, W.T. Sheng, W. Guo, S.Y. Qiu, J. Deng and X. Wang, "Dynamic parameter identification of a lower extremity exoskeleton using RLS-PSO," Appl. Sci.-Basel, vol. 9, pp. 1-17, 2019.

[16] Y. Sahin, F.M. Botsali, M. Kalyoncu, M. Tinkir, U. Onen, N. Yilmaz, O.K. Baykan, A. Cakan, "Force feedback control of lower extremity exoskeleton assisting of load carrying human," *Advanced Materials, Mechanics and Industrial Engineering*, pp. 546-550, 2014.

[17] Y. Sahin, F.M. Botsali, M. Kalyoncu, M. Tinkir, U. Onen, N. Yilmaz, A. Cakan, "Mechanical design of lower extremity exoskeleton assisting walking of load carrying human, Advanced Materials," *Mechanics and Industrial Engineering*, pp. 141-145, 2014.

[18] S. Ding, X.P. Ouyang, T. Liu, Z.H. Li, H.Y. Yang, "Gait event detection of a lower extremity exoskeleton robot by an intelligent IMU," *IEEE Sens. J.*, vol. 18, pp. 9728-9735, 2018.

[19] G. Chen, P. Qi, Z. Guo, H.Y. Yu, "Mechanical design and evaluation of a compact portable knee-ankle-foot robot for gait rehabilitation," *Mech. Mach. Theory*, vol. 103, pp. 51-64, 2016.

[20] R. Singh, H. Chaudhary, A.K. Singh, "A novel gait-based synthesis procedure for the design of 4-bar exoskeleton with natural trajectories," *J. Orthop. Transl.*, vol. 12, pp. 6-15, 2018.

[21] C.T. Farley, H.H.P. Houdijk, C. Van Strien, M. Louie, "Mechanism of leg stiffness adjustment for hopping on surfaces of different stiffnesses," *J. Appl. Physiol.*, vol. 85, pp. 1044-1055, 1998.

[22] H. Hobara, K. Inoue, T. Muraoka, K. Omuro, M. Sakamoto, K. Kanosue, "Leg stiffness adjustment for a range of hopping frequencies in humans," *J. Biomech.*, vol. 43, pp. 506-511, 2010.

[23] J.F. Veneman, R. Kruidhof, E.E.G. Hekman, R. Ekkelenkamp, E.H.F. Van Asseldonk, H. van der Kooij, "Design and evaluation of the LOPES exoskeleton robot for interactive gait rehabilitation," *IEEE Trans. Neural Syst. Rehabil. Eng.*, vol. 15, pp. 379-386, 2007.

[24] M. Cestari, D. Sanz-Merodio, J.C. Arevalo, E. Garcia, "An Adjustable Compliant Joint for Lower-Limb Exoskeletons," *IEEE-ASME Trans. Mechatron.*, vol. 20, pp. 889-898, 2015.

[25] D. Rodriguez-Cianca, C. Rodriguez-Guerrero, T. Verstraten, R. Jimenez-Fabian, B. Vanderborght, D. Lefeber, "A Flexible shaft-driven Remote and Torsionally Compliant Actuator (RTCA) for wearable robots," *Mechatronics*, vol. 59, pp. 178-188, 2019.

[26] H. Aguilar-Sierra, W. Yu, S. Salazar, R. Lopez, "Design and control of hybrid actuation lower limb exoskeleton," *Adv. Mech. Eng.*, vol. 7, pp.1-13, 2015.

[27] M.D. Sanchez-Villamanan, J. Gonzalez-Vargas, D. Torricelli, J.C. Moreno, J.L. Pons, "Compliant lower limb exoskeletons: a comprehensive review on mechanical design principles," *J. NeuroEng. Rehabil.*, vol.16, 1-16, 2019.

[28] Y. Long, Z.J. Du, C.F. Chen, W.D. Wang, W. Dong, "Development of a lower extremity wearable exoskeleton with double compact elastic module: preliminary experiments," *Mech. Sci.*, vol. 8, pp. 249-258, 2017.

[29] B. Bigge and I.R. Harvey, "Programmable springs: Developing actuators with programmable compliance for autonomous robots," *Robot. Auton. Syst.*, vol. 55, pp. 728-734, 2007.

[30] S. Krut, M. Benoit, E. Dombre, F. Pierrot, MoonWalker, "A lower limb exoskeleton able to sustain bodyweight using a passive force balancer," *IEEE International Conference On Robotics and Automation*, pp. 2215–2220, 2010.

[31] H. Kawamoto, S. Lee, S. Kanbe, Y. Sankai, "Power assist method for HAL-3 using EMG-based feedback controller," *IEEE International Conference on Systems, Man and Cybernetics*, pp. 1648-1653, 2003.

[32] K.A. Strausser, T.A. Swift, A.B. Zoss, H. Kazerooni, "Prototype medical exoskeleton for paraplegic mobility: first experimental results," *ASME 2010 Dynamic Systems and Control Conference*, pp.1-6, 2010.

[33] J. Beil, G. Perner and T. Asfour, "Design and control of the lower limb exoskeleton KIT-EXO-1," *International Conference on Rehabilitation Robotics*, pp. 119-124, 2015.

[34] J.F. Veneman, R. Ekkelenkamp, R. Kruidhof, F.C.T. van der Helm, H. van der Kooij, "Design of a series elastic- and Bowdencable-based actuation system for use as torque-actuator in exoskeleton-type training," *IEEE 9th International Conference on Rehabilitation Robotics*, New York, pp. 496-499, 2005.

[35] S. Wang, C. Meijneke, H. van der Kooij, "Modeling, design, and optimization of Mindwalker series elastic joint," *IEEE International Conference on Rehabilitation Robotics*, 2013